Cableless Battery Charger Using Induction Technique for Electric Vehicles

Nasrul Humaimi Mahmood, Mohamed Amin Alias, Mohd Wazir Mustapha, Mazlina Esa and Faridah Taha
Cordless Charger Research Group
Faculty of Electrical Engineering, Universiti Teknologi Malaysia
81300 UTM Skudai, Johor, Malaysia
e-mail: nasrul@suria.fke.utm.my

Abstract- Electromagnetic induction is the production of an electromotive force in a conductor as a result of a changing magnetic field about the conductor. The induced emf always such that it opposes the change that gives rise to it, according to Lenz's law. In our work, we are considering in controlling the magnetic flux distribution through an air-gap during the energy transfer from the source to load. This research has put a core situation in investigating the possible ways of charging the batteries via mutual induction as in transformers. This enables the charging process to be cableless. It involves two coils transferring energy from one to the other through air in the most efficient way. Our work is presented in this paper. Simulation and hardware implementation has been carried out successfully. We have measured the magnetic flux density for ac input voltage of 100 Volt with different frequency values. The optimum frequency in our design is 25 Hz. We found that it is possible to control the magnetic flux distribution during energy transmission by optimizing the frequency and shielding the flux path.

Keywords
Cordless charger, induction, magnetic flux control.

I. INTRODUCTION

The work described in this report is an alternative charging of the battery for electric vehicles. In our work, we introduce the charging method to be cableless since without connector, we can safe our time of plugging the connector and this will be more efficient. We can build a parking lot with the primary coil embedded in a parking lot, which provide magnetic field as a medium of energy transfer to charge the electric vehicle's battery. The secondary coil is mounted on electric vehicles and received the energy from primary coil via mutual inductance. This charging method is suitable for shopping complex's car park and other places which require a big space of parking lots.

The investigation of charging the battery via mutual induction as in transformer is divided into software simulation and hardware implementation. We used Finite Element Method Magnetic software (FEMM ver 3.1) for the simulation work while the experiments have been done in R&D Electronics laboratory at Faculty of Electrical Engineering, UTM.

II. SOFTWARE IMPLEMENTATION

FEMM 3.1 software is very useful in modeling the magnetic flux distribution for different shape of core. We developed five optimum samples of the design with contour and density plots. One of the most useful ways to understand the magnetic finite element solution is by plotting the "flux lines". These are streamlines along which flux flows in the finite element geometry. When flux lines are close together, the flux density is high. From the design, the primary and secondary cores are integrated to visualise the magnetic field energy for both cores. The small difference in values indicates that the design is possible to transfer the energy with low losses. Figure 1 (a) to (e) explain the pattern of magnetic flux distributions for different designs of core shapes.

From all the patterns, it can be seen that the shape of the core plays an important role in determining the magnetic flux lines distributions. For example, compare pattern 1 and pattern 2. If we make the ends of both the primary and secondary cores as concave surfaces, the magnetic flux lines converge from the end part of primary and secondary. As the magnetic flux lines decrease, this will give better results since we can reduce the losses. However, there are still a lot of joint flux lines between the end part of primary which can reduce the output voltage at secondary coils. To solve this, we need to increase the distance between the end parts of each core as shown in Figure 1(c). As a result, we can see that the joint magnetic flux lines decreases and this will make sure that more magnetic flux from primary is induced into the secondary part.

Figure 1(d) and (e) are the effects of magnetic flux lines distribution as we decrease the size of the end part of the primary compared to the secondary end part. From the density plot (Tesla), we can see that more magnetic flux lines from the primary part enter the secondary part of the core and this shows us that by decreasing the primary shape, we can get better results compared to others.

To make clear which is the best pattern that we are going to use later, we integrate the primary and secondary part for each patterns and find the minimum losses during the energy transmission. The lowest percentage of losses will give better results of possible

0-7803-8173-4/03/$17.00 ©2003 IEEE.

way to control the magnetic flux distribution through an air gap. The air gap for all patterns is 4 cm.

The corresponding losses of magnetic field energy are tabulated in Table 1. From the table, pattern 5 produces the smallest percentage of losses while pattern 1 produces the highest percentage of losses compared to other patterns. Figure 2 shows the percentage distribution in pie form. This means that the better solution for the optimum core shape design is by making the end part of the primary core as a convex surface while the secondary as the concave surface. It is also better to increase the distance between the end part of both the primary and secondary cores since the percentage of the losses in pattern 2 decreases dramatically compared to the losses in pattern 3 from 56.27 % to 39.4 %.

By reducing the angle of the end part of the primary (pattern 5), better results are achieved. As we increase the angle of convex surface from 20^{O} to 40^{O}, the percentage of losses reduce from 36.7 % to 36.2 %. This is given in Table 2. Therefore, to achieve the optimum result, we also need to consider the surface angle of the end part of the core.

III. HARDWARE IMPLEMENTATION

The hardware implementation begins with constructing the design of the core based on its shape which has been simulated by the FEMM 3.1 software. The core design is sent to the iron engineering company for construction. The next step is setting up of the apparatus for controlling the magnetic flux distribution.This apparatus include the source,autotransformer (VARIAC) to select the suitable voltage for the used current, the designed core, the enameled-copper wire as the coils to produce the electromagnetic field, the power amplifier devices to increase the strength of the frequency, frequency generator and flux meter for measuring the magnetic flux density and strength. Figure 3 shows the experimental setup in the R & D Electronic laboratory (UTM).

We have two parts of experimental setup. The first part is to find the suitable voltage and current for the design by adjusting the VARIAC (autotransformer). We are finding the optimum current for the supply voltage. The second part is used to find the optimum frequency for our design by adjusting the frequency generator, which is connected to the power amplifier. By looking the voltage changing at secondary core, we found the optimum frequency of our design. Flux meter used in both experimental setups measure the magnetic flux density (in Tesla) From the measured values, we can draw the magnetic flux lines path by finding the same range of values.

IV. RESULTS AND ANALYSIS

A. Effect of the air gap

Firstly, the effect of the air gap to the output voltage for different input voltages is investigated. The input and output voltages are measured in Volts, V (AC Source). The air gap here is defined as the gap between the ending parts of each core. For each air gap, we measure the output voltage (induced voltage) at the secondary core according to the different primary input voltage. It was found that, as the length of the air-gap is increased, the output voltage is decreased. This means that it is quite difficult to control the magnetic flux distribution when the air gap is increased. This is a challenge for us to solve this problem to en sure that we achieve the optimum voltage induced in the secondary part to increase the efficiency. This conclude that the shape of the core is very important in determining a possible way of controlling the magnetic flux during energy transmissions.

We measure the length of the air-gap and its corresponding output voltage (secondary coils) for a given fixed input voltage (primary coils) of 50 V. The result is tabulated in Table 3 and plotted in Figure 4.

B. Effect of magnetic shielding

As described in Section III, we measure the magnetic flux density using the magnetic flux meter by putting the probe between the primary and secondary cores. The value of flux lines are obtained by moving the probe. The flux lines are then drawn. From the experiment, it was found that the magnetic flux lines tend to converge into straight lines to the end part of the secondary core which will reduce the energy losses when we use an aluminum for shielding the back of the secondary end part. The magnetic flux density is measured in mT.

C. Optimum frequency of the design

To find the optimum frequency for our design, we adjust the frequency generator, which is connected to the power amplifier. By measuring the voltage change at the secondary coils, we deduced the optimum frequency of our design. At the beginning, we set the frequency at 50 Hz and the input voltage is connected to the power amplifier at 0.466 V. Then we measure the output voltage at the secondary turns. After that, we increase the frequency slowly up to 80 Hz and also decrease the frequency until 0 Hz. The output voltage measured at the secondary coils for different frequencies are tabulated in Table 4.

From Table 4, it can be seen that the output voltage starts to drop at a frequency of 20 Hz. This means that 20 Hz is the optimum frequency achieved. This is also illustrated in Figure 5.

From Figure 5, the output voltage at 50 Hz is 0.31 V. When we increase the frequency, the voltage slightly

decreases. When we decrease the frequency, the output voltage at the secondary coils increases. However, when the frequency value reaches Hz, the output voltage does not change until it starts to drop back at the frequency of 15 Hz. From here we can conclude that the voltage starts to drop at 20 Hz which means that this is the optimum frequency achieved. This frequency depends on the material used, coils windings and number of turns. Different core shape design gives different values of optimum frequency. Based on our observation, by reducing the number of turns, the optimum frequency will increase.

V. CONCLUSION

This paper has proposed a method of controlling the magnetic flux distribution during the energy transmission from the primary to secondary coil through an air-gap. The results presented in this paper indicate that:

(i) the optimum design shape of the core has to ensure that we can operate with low energy losses during energy transmission. This can be done by making the end part of the primary core as a convex surface and the secondary core as a concave surface.

(ii) by shielding the part of the flux path at the core, we can get better flux lines distribution, which concentrate to each other.

(iii) from the simulations carried out, it is better to increase the distance between the end part of each core to ensure lots of magnetic flux from the primary core will converge to the secondary core.

(iv) the effect of the optimum frequency depends on the material used as the core, the number of turns and the methods of coil windings.

VI. ACKNOWLEDGEMENTS

The work carried out is funded by IRPA grant vote 72356.

VII. REFERENCES

[1] D.Bruce Montgomery, "Iron Magnet Design", 1961, Proceeding on High magnetic field.

[2] David Dugdale, "Essential of Electromagnetism", 1993, The Macmillan Press Limited.

[3] David Meeker, "Finite Element Method Magnet IC-Software Manual Book", 2000, http://members.aol.com/dcm3c

[4] I. Marinova, S Hayano and Y.Saito, "Inverse approach for shape design of magnetic core", 1995, IEEE Trans. On Magnet.

[5] Masato Enokizono and Takashi Tokada, "Flux controlling Method of Magnetic Circuit and its application", 1993, IEEE Trans. On Magnetics.

[6] Nasir hassan Kutkut, " An electric vehicle battery charging system", 1995, Dissertation Abstract, University of Wisconsin.

[7] P.D Barbar, P Navarra, A savini, R Sikora, "Optimum design of iron-core electromagnets", 1990, IEE Trans. On Magnetics.

[8] William M Flanagan, " Handbook of transformer applications", 1986, Mc Graw Hill Book Company.

[9] William Manuel, " Inductive Charging of moving electric vehicle", 1995, Dissertation Abstract, UMI.

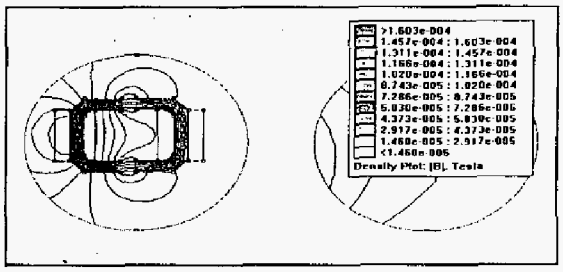

(a) pattern 1

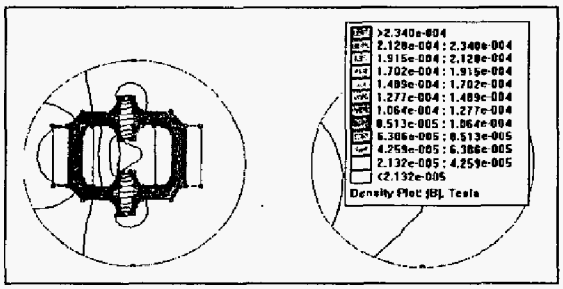

(b) pattern 2

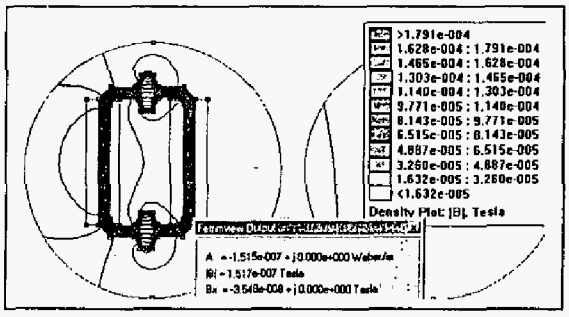

(c) pattern 3

Figure 1. Different patterns of magnetic flux lines distribution with its density plot for different core shape designs.

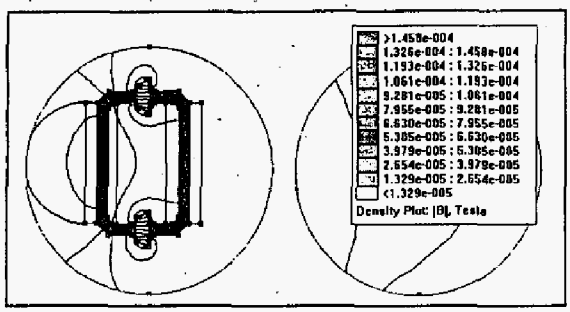

(d) pattern 4

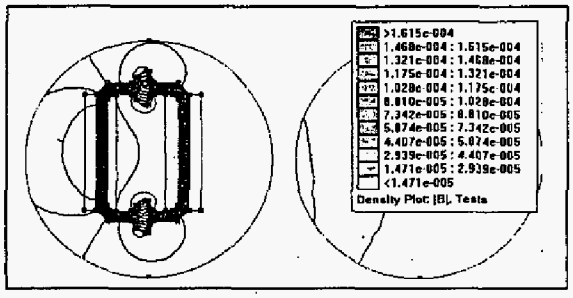

(e) pattern 5

Figure 1. Different patterns of magnetic flux lines distribution with its density plot for different core shape designs (contd.)

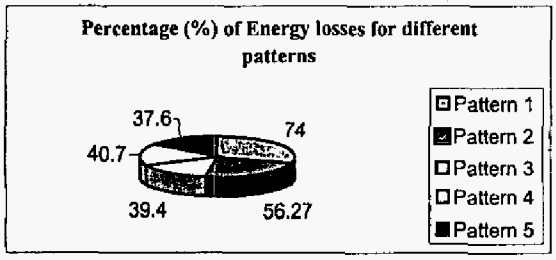

Figure 2. Percentage of energy losses for different magnetic flux lines distribution patterns.

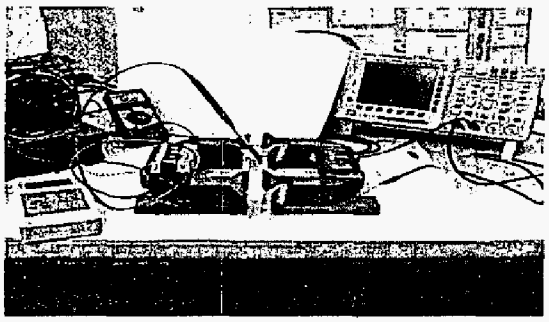

Figure 3. Experimental set-up in R&D Electronic laboratory in UTM.

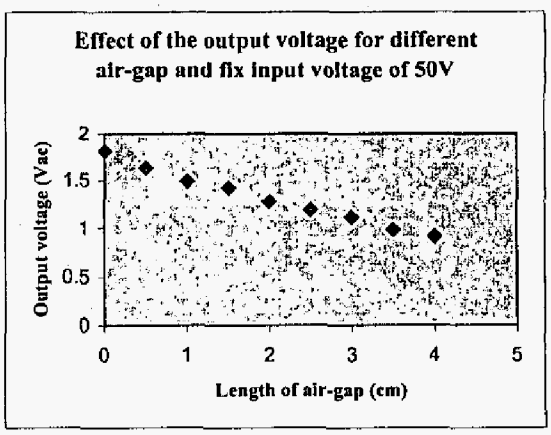

Figure 4. Effect of output voltage for different air gaps and fixed input voltage of 50 V.

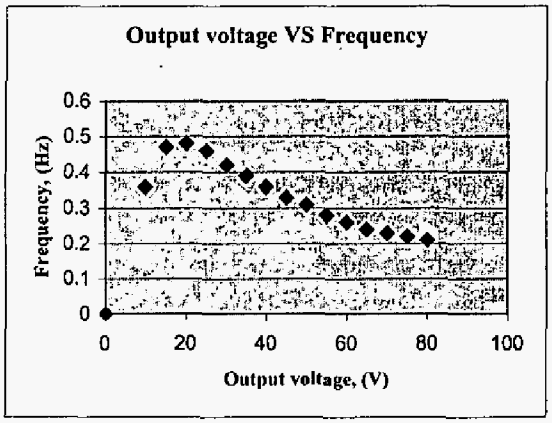

Figure 5. Effect of the secondary coils output voltage at different frequencies.

Table 1. Losses of magnetic field energy for each pattern of magnetic flux lines distribution.

	Primary, x 10^{-9}J/m	Secondary, x 10^{-9}J/m	Energy Losses, J/m	Losses %
Pattern 1	9.22	2.397	6.83	74
Pattern 2	21.62	9.67	11.95	56.27
Pattern 3	29.330	17.759	11.561	39.40
Pattern 4	17.269	10.232	7.03	40.70
Pattern 5	20.432	12.747	7.685	37.60

Table 2. Magnetic field energy losses for different surface angle in Pattern 5.

Angle, degree	Primary, x 10^{-9}J/m	Secondary, x 10^{-9}J/m	Energy Losses, J/m	Losses, %
20	20.4315	12.7465	7.6849	7.60
30	22.0335	13.9737	8.0598	36.50
40	14.2765	14.2765	8.1292	36.20

Table 3. Effect of the output voltage for different air-gaps and fixed input voltage of 50 V.

Length of the air-gap (cm)	Output voltage, V_{out} (V_{ac})
0	1.81
0.5	1.63
1.0	1.49
1.5	1.42
2.0	1.28
2.5	1.19
3.0	1.11
3.5	0.98
4.0	0.91

Table 4. Effect of the frequencies to the secondary coils output voltages.

Frequency (Hz)	**Secondary coils output voltage (V)**
0	0
10	0.36
15	0.47
20	0.48
25	0.46
30	0.42
35	0.39
40	0.36
45	0.33
50	0.31
55	0.28
60	0.26
65	0.24
70	0.23
75	0.22
80	0.21